

Research Article

# Quantum Tunneling in Breather ‘Nano-colliders’

V.I. Dubinko\*

*NSC Kharkov Institute of Physics and Technology, 1 Akademicheskaya St., Kharkov 61108, Ukraine*

---

## Abstract

In many crystals with sufficient anharmonicity, special kinds of lattice vibrations, namely, discrete breathers (DBs) can be excited either thermally or by external triggering, in which the amplitude of atomic oscillations greatly exceeds that of harmonic oscillations (phonons). Coherency and persistence of large atomic oscillations in DBs may have drastic effect on quantum tunneling due to *correlation effects* discovered by Schrödinger and Robertson in 1930. These effects have been applied recently to the tunneling problem by Vysotskii et al., who demonstrated a giant increase of sub-barrier transparency during the increase of the correlation coefficient at special high-frequency periodic action on the quantum system. In the present paper, it is argued that DBs present the most natural and efficient way to produce correlation effects due to time-periodic modulation of the potential well width (or the Coulomb barrier width) and hence to act as breather ‘nano-colliders’ (BNC) triggering low energy nuclear reactions (LENR) in solids. The tunneling probability for deuterium (D–D) fusion in ‘gap DBs’ formed in metal deuterides is shown to increase with increasing numbers of oscillations by  $\sim 190$  orders of magnitude, resulting in the observed LENR rate at extremely low concentrations of DBs. Possible ways of engineering the nuclear active environment based on the present concept are discussed.

© 2016 ISCMNS. All rights reserved. ISSN 2227-3123

*Keywords:* Correlation effects, Discrete breathers, Low energy nuclear reactions, Nuclear active sites

---

## 1. Introduction

The problem of tunneling through the Coulomb potential barrier during the interaction of charged particles is the key to modern nuclear physics, especially in connection with low energy nuclear reactions (LENR) observed in solids [1–4].

The tunneling (a.k.a. transmission) coefficient (TC) first derived by Gamow (1928) for a pure Coulomb barrier is the Gamow factor, given by

$$G \approx \exp \left\{ -\frac{2}{\hbar} \int_{r_1}^{r_2} dr \sqrt{2\mu (V(r) - E)} \right\}, \quad (1)$$

where  $2\pi\hbar$  is the Planck constant,  $E$  is the nucleus CM energy,  $\mu$  is the reduced mass,  $r_1, r_2$  are the two classical turning points for the potential barrier, which for the D–D reaction are given simply by  $\mu = m_D/2$ ,  $V(r) = e^2/r$ .

---

\*E-mail: vdubinko@hotmail.com

For two D's at room temperature with thermal energies of  $E \sim 0.025$  eV, one has  $G \sim 10^{-2760}$ , which explains the pessimism about LENR and shows the need for some special conditions arising in solids under typical LENR conditions ( $D_2O$  electrolysis [1–3], E-cat [4], etc.), which help to overcome the Coulomb potential.

Corrections to the cross section of fusion due to the screening effect of atomic electrons result in the so-called “screening potential”, which acts as additional energy of collision at the center of mass [5]. The screening potential was measured by the yields of protons or neutrons emitted in the  $D(d, p)T$  or  $D(d, n)^3He$  reactions induced by bombardment of D-implanted solid targets with deuterons accelerated to kinetic energies of several keV, equivalent to heating up to  $\sim 10^7$  K [6]. However, even the maximum screening potentials found in Pt (675 eV), PdO (600 eV) and Pd (310 eV) are far too weak to explain LENR observed at the temperatures of these experiments, which are below the melting point of solids (in the E-cat) or boiling point of liquids (with electrolysis). Besides, the absence of significant radiation under typical LENR conditions indicates that other reactions should take place, based on interactions between ‘slow’ particles, which may be qualitatively different from the interactions between accelerated ones.

The most promising and universal mechanism of the stimulation of nuclear reactions running at low energy is connected with the formation of *coherent correlated states* of interacting particle, which ensures the high probability of the nuclear reactions under conditions, where the ordinary tunnel effect is negligible. These states minimize a more general uncertainty relation (UR) than Heisenberg UR usually considered in quantum mechanics, namely, Schrödinger–Robertson UR [7,8], which takes into account correlations between coordinate and momentum operators. Correlation effects have been applied to the tunneling problem by Dodonov et al. [9] and more recently by Vysotskii et al. [10–13] who demonstrated a giant increase of sub-barrier transparency (up to hundreds of orders of magnitude!) during the increase of correlation coefficient at special high-frequency periodic action on quantum system.

In this paper, we argue that such an action can be most naturally and effectively realized due to time-periodic modulation of the width of potential wells for atoms oscillating in the vicinity of discrete breathers (DBs). DBs are spatially localized large-amplitude vibrational modes in lattices that exhibit strong anharmonicity [14–23]. Due to the crystal anharmonicity, the frequency of atomic oscillations increase or decrease with increasing amplitude so that the DB frequency lies outside the phonon frequency band, which explains the weak DB coupling with phonons and, consequently, their robustness at elevated temperatures. DBs can be excited either thermally or by external driving, as was observed experimentally [17,18] and modelled in various physical systems [19–24].

Studies of DBs in three-dimensional crystals by means of molecular dynamics simulations using realistic interatomic potentials include ionic crystals with NaCl structure [16,19,20], diatomic  $A_3B$  crystals [21], graphene [22], semiconductors [23] and metals [24,25]. DBs in biopolymers such as protein clusters have been studied using the coarse-grained nonlinear network model [26].

Presently the interest of researchers has shifted to the study of the *catalytic impact* of DBs on the reaction rates in solids and on the biological functions of biopolymers [26,27]. The excitation of DBs in solids have been shown to result in a drastic amplification of the reaction rates in their vicinity. Two cases considered up to now include chemical reactions [27–30] and LENR [31]. In the former case, the amplification mechanism is based on modification of the classical Kramers escape rate from a potential well due to a periodic modulation of the well depth (or the reaction barrier height), which is an archetype model for chemical reactions since 1940 [27].

In the latter case, the so-called *gap DBs*, which can arise in diatomic crystals such as metal hydrides/deuterides (e.g. palladium deuteride, PdD), have been argued to be the LENR catalyzers [31]. The large mass difference between H or D and the metal atoms provides a gap in the phonon spectrum, in which DBs can be excited in the H/D sub-lattice resulting in time-periodic closing of adjacent H/D atoms, which should enhance their fusion probability. The main problem with this mechanism was that unrealistically small separation between atoms ( $\sim 0.01$  Å) must be attained in order to increase TC (Eq. (1)) by  $\sim 100$  orders of magnitude required for a noticeable LENR rate at the best choice of parameters. Such distances are considerably smaller than the range of conventional chemical forces. However, this estimate did not take into account correlations between coordinate and momentum operators arising in a DB due to the

cooperative nature of its dynamics. This problem is addressed in the present paper.

This paper is organized as follows. In Section 2, formation of coherent correlated states (CCS) under time-periodic action on a particle in the parabolic potential is reviewed [11–13]. In Section 3, this model is applied to the evaluation of the TC for the atoms oscillating in the vicinity of DBs and of the corresponding increase of their fusion rate. In Section 4, based on the rate theory of DB excitation under D<sub>2</sub>O electrolysis and on the modified TC for D–D fusion in the PdD lattice, the fusion energy production rate is evaluated as a function of temperature, electric current and material parameters and compared with experimental data. The results are summarized in Section 5.

## 2. Formation of Correlated States in Non-stationary Potential Well

### 2.1. Schrödinger–Robertson UR and TC

The tunneling effect for nuclear particles is closely related to the uncertainty relation (UR), which determines the limits of the applicability of the classical and quantum descriptions of the same object. It appears that the well-known and widely used Heisenberg UR is a special case of a more general inequality, discovered independently by Schrödinger [7] and Robertson [8], which can be written in the following form [9]

$$\sigma_x \sigma_p \geq \frac{\hbar^2}{4(1-r^2)}, \quad \sigma_x = \left\langle \left( x - \langle x \rangle \right)^2 \right\rangle, \quad \sigma_x = \left\langle \left( p - \langle p \rangle \right)^2 \right\rangle, \quad (2)$$

where

$$r = \frac{\sigma_{xp}}{\sqrt{\sigma_x \sigma_p}}, \quad \sigma_{xp} = \langle \hat{x} \hat{p} + \hat{p} \hat{x} \rangle / 2 - \langle x \rangle \langle p \rangle \quad (3)$$

is the *correlation coefficient* between the coordinate,  $x$ , and momentum,  $p$ . At  $r = 0$  (non-correlated state) Eq. (2) is reduced to the Heisenberg UR, while in a general case, a non-zero  $r$  in the UR can be taken into account by the formal substitution

$$\hbar \rightarrow \hbar_{\text{ef}} = \frac{\hbar}{\sqrt{1-r^2}}, \quad (4)$$

which leads to the formal shift of the border between the classical and quantum descriptions of the same object in the transition from non-correlated to correlated state [13].

Given this, a natural question arises: can nonzero correlations lead to real physical effects? If yes, then the most impressive consequence would be a dramatic increase of the tunneling probability, if a true Planck constant in Eq. (1) could be replaced by the effective parameter (4). This substitution was justified by Vysotskii et al. [10–13], who solved the non-stationary Schrödinger equation for the particle wave function  $\psi(x, t)$  with account of correlation effects for a very low barrier transparency (tunneling probability) in the initially uncorrelated state  $G_{r=0} \ll 1$  that corresponds to the condition  $E \ll V_{\text{max}}$ :

$$G_{r \neq 0} \approx \exp \left\{ -\frac{2}{\hbar_{\text{ef}}} \int_{r_1}^{r_2} dr \sqrt{2\mu(V(r) - E)} \right\} = (G_{r=0})^{\sqrt{1-r^2}}. \quad (5)$$

This approximation is within an order of magnitude of the result of the exact calculation of the potential barrier transparency using rigorous quantum-mechanical methods [10–13]. From Eq. (5), it follows that when a strongly correlated state with  $|r| \rightarrow 1$  is formed, the product of the variances of the particle coordinate and momentum increases indefinitely, and the barrier becomes ‘transparent’:  $G_{|r| \rightarrow 1} \rightarrow 1$  even if  $E \ll V_{\text{max}}$ .

Although the substitution  $\hbar \rightarrow \hbar_{\text{ef}}$  is not quite correct, it clearly demonstrates the high efficiency of using coherent correlated states in solving applied tunneling-related problems in the case of a high potential barrier and a low particle energy  $E \ll V_{\text{max}}$ , which is typical for LENR.

CCS can be formed in various quantum systems. The most natural way to form such state is to place a particle in a *non-stationary potential well*.

## 2.2. Formation of CCS under time-periodic oscillation of harmonic potential well

A model system considered by Vysotskii et al. [11–13], for the evaluation of the correlation coefficient, is a particle with the mass  $M$ , coordinate  $x(t)$  and momentum  $p(t)$  in a non-stationary parabolic potential well (i.e. non-stationary harmonic oscillator),

$$V(x, t) = M(x(t))^2(\omega(t))^2/2 \tag{6}$$

for which a change of the eigen frequency  $\omega(t)$  was shown to result in an increase of  $|r(t)|$ . Several scenarios of time evolution  $\omega(t)$  have been investigated [11–13], including its monotonic decrease or periodic modulation. The latter regime can be provided, e.g. at a constant well depth  $V_{\text{max}}$  and the potential well width  $L(t)$  that changes periodically resulting in a time-periodic modulation of the eigen frequency as follows:

$$L(t) = L_0(1 + g_\Omega \cos \Omega t), \quad L_0 = \sqrt{8V_{\text{max}}/M\omega_0^2}, \tag{7}$$

where  $L_0$  and  $\omega_0$  are the initial parameters of the well before the action of correlated forces,  $g_\Omega$  and  $\Omega$  are the modulation amplitude and frequency, respectively.

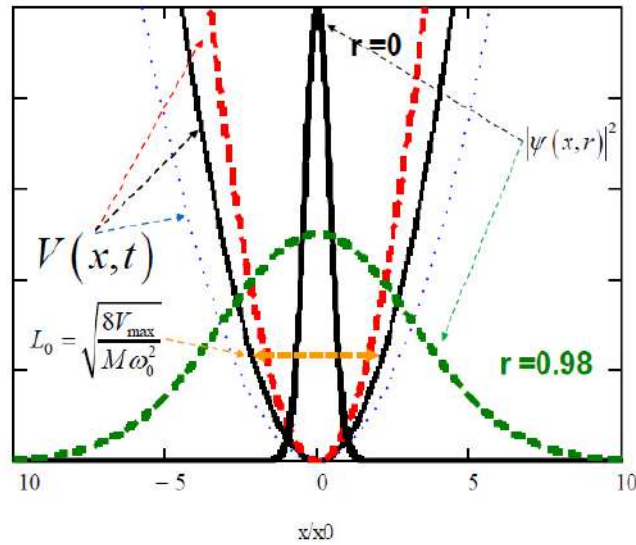


**Figure 1.** Sketch of the time-periodic parabolic potential  $V(x, t)$  at different moments of time corresponding to the initial (solid black), minimal (dash red) and maximal (dot blue) well width. Probability density  $|\psi(x, r)|^2$  for the particle localization in the well and in the sub-barrier region is shown schematically for uncorrelated state  $r = 0$  (solid black) and for strongly correlated state  $r = 0.98$  at the times of the maximal coordinate dispersion (dash green) [10].  $x_0 = \sqrt{\hbar/M\omega_0^2}$  is the half-width of the particle localization in the unperturbed well.

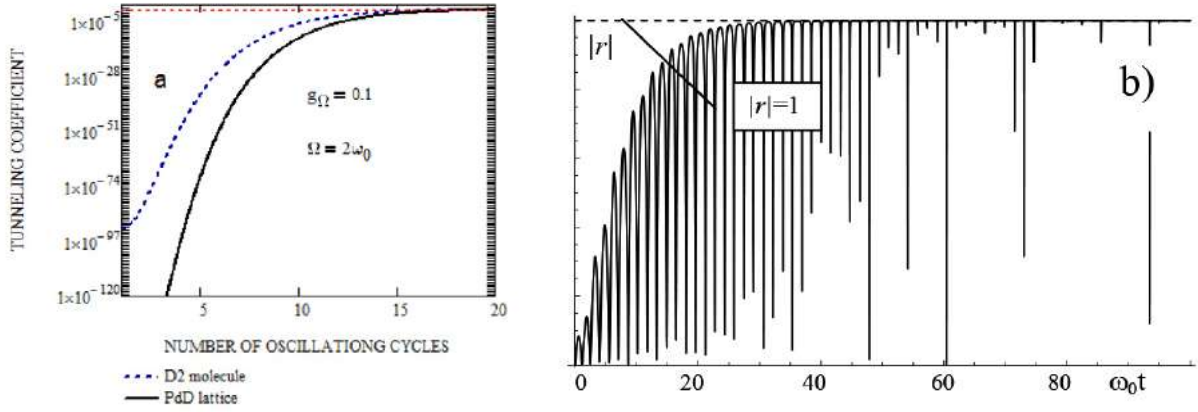


**Figure 2.** (a) Tunneling coefficient increase with increasing number of the well modulation cycles,  $n = \omega_0 t / 2\pi$ , evaluated by Eq. (8) for the correlation coefficient amplitude increasing as shown in (b) at  $\Omega \approx 2\omega_0$ ,  $g_\Omega = 0.1$  [13]. D–D equilibrium spacing in a  $D_2$  molecule ( $L_0 = 0.74 \text{ \AA}$ ) and in the PdD crystal ( $L_0 = 2.9 \text{ \AA}$ ).

Figure 1 shows that the probability density  $|\psi(x, r)|^2$  for the particle localization in the time-periodic well is very narrow for uncorrelated state  $r = 0$  (solid black), while it spreads significantly into the sub-barrier region for the strongly correlated state  $r = 0.98$  at the times of the maximal coordinate dispersion (dash green) [10].

From a detailed analysis [11–13] it follows that the process of formation of strongly correlated coherent state with  $|r|_{\max} \rightarrow 1$  in response to the action of limited periodic modulation (Eq. (10)) is possible only at any of two conditions: (i)  $\Omega = \omega_0$  (resonant formation) or (ii)  $\Omega$  is close to  $2\omega_0$  (parametric formation):  $|\Omega - 2\omega_0| \leq g_\Omega \omega_0$ .

Figure 2 shows the evolution of the correlation coefficient in time under the action of the harmonic perturbation with a parametric frequency  $\Omega = 2\omega_0$  at  $g_\Omega = 0.1$ . The correlation coefficient oscillates with time but its amplitude  $|r|_{\max}$  increases monotonically with the number of modulation cycles,  $n = \omega_0 t / 2\pi$ , resulting in a giant increase of the tunneling coefficient, as demonstrated in Fig. 3, which shows the TC evaluated by Eq. (8) that takes into account both the electron screening [31] and the correlation effects [13]:

$$G^*(L, r) = \exp \left\{ -\frac{2\pi e^2}{\hbar_{\text{ef}}(r)} \sqrt{\frac{\mu}{2(E + e^2/L)}} \right\}, \quad (8)$$

where  $L$  is the minimum equilibrium spacing between D atoms determined by electron screening,  $E$  is their kinetic energy ( $\sim eV/40$  at room temperature)  $\ll$  screening energy  $\sim e^2/L$ . One can see that the difference in electron screening and the corresponding initial D–D distances in a  $D_2$  molecule ( $L_0 = 0.74 \text{ \AA}$ ) and in the PdD crystal ( $L_0 = 2.9 \text{ \AA}$ ) leads to a huge tunneling difference in the initial (uncorrelated) state, in which TC is negligible in both cases. However, with increasing number of modulation cycles, the correlation coefficient amplitude increases according to Fig. 2 resulting in a giant increase of TC up to  $\sim 1$  in dozens of cycles for parametric formation  $\Omega \approx 2\omega_0$ , which does not require an exact coincidence of the frequencies [13].

The most important and non-trivial practical question now is: how to realize such a periodic action at the atomic scale? Modulation of the frequency of the optical phonon modes via excitation of the surface electron plasmons by a terahertz laser suggested in [13] as a driving force for the CCS formation is very questionable [31], and it does not explain LENR observed in the absence of laser driving. In Section 3, we will consider a new mechanism based on the large-amplitude time-periodic oscillations of atoms naturally occurring in discrete breathers.

### 3. Breather-induced Time-periodic Action on the Potential Barrier

In order to develop a mechanism for DB-based LENR in metal hydrides/deuterides (e.g. PdD or NiH), let us consider their crystal structure in more detail. At ambient conditions, Ni/Pd hydrides/deuterides crystallize in FCC structure with the space group of the Rock-salt structure, which is called Fm3m in Hermann–Mauguin notation [32,33].

Molecular dynamic (MD) simulations have revealed that diatomic crystals with Morse interatomic interactions typically demonstrate *soft type* of anharmonicity [19], which means that DB's frequency decreases with increasing amplitude, and one can expect to find the so-called gap DBs with a frequency within the phonon gap of the crystal. The large mass difference between H or D and the metal atoms is expected to provide a wide gap in phonon spectrum (Fig. 3), in which DBs can be excited, e.g. by thermal fluctuations at elevated temperatures, as demonstrated by Kistanov and Dmitriev [20] for the different weight ratios and temperatures. The density of phonon states (DOS) of the NaCl-type crystal for the weight ratio  $m/M = 0.1$  at temperatures ranging from 0 to 620 K is shown in Fig. 3 (a)–(d).

Figure 3 (e) shows that DOS for PdD and PdH measured experimentally are qualitatively similar to DOS calculated for the NaCl-type crystal. First-principle calculations [33] point out that phonon spectra in PdD and PdH are strongly renormalized by anharmonicity. The appearance of two additional broad peaks in the DOS of NaCl at elevated temperatures (starting from  $T = 310$  K) can be seen in Fig. 3 (c), (d). One of them is in the gap of the phonon spectrum, while another one lies above the phonon spectrum. The appearance of the peak *in the gap* of the phonon spectrum can be associated with the spontaneous excitation of gap DBs at sufficiently high temperatures, when nonlinear terms in the expansion of interatomic forces near the equilibrium atomic sites acquire a noticeable role. As the temperature increases, the lifetime and concentration of gap DBs in the *light atom sub-lattice* increase [21]. The dynamic structure of gap DBs has been revealed in [19] where they have been excited simply by shifting one *light atom* or two neighboring light atoms from their equilibrium positions while all other atoms were initially at their lattice positions and had zero initial velocities.

There are two main peculiarities of DBs related to the formation of coherent correlated states, namely, oscillations of atoms comprising a DB are (i) *time-periodic* and (ii) *coherent*, i.e. they have different amplitudes but the same or

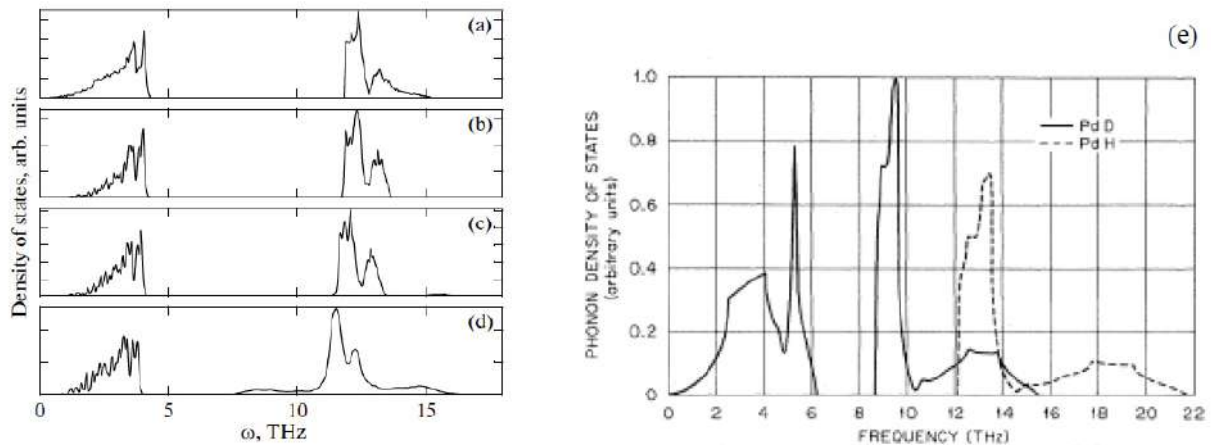


**Figure 3.** DOS of the NaCl-type crystal for the weight ratio  $m/M = 0.1$  at temperatures  $T =$ (a) 0, (b) 155, (c) 310, and (d) 620 K. (e) DOS for PdD and PdH crystals based on the force constants [33] fitted to the experimental results for PdD<sub>0.63</sub> assuming that the forces in PdD and PdD<sub>0.63</sub> were identical. Reproduced from [20,33] Copyright by APS.

commensurate frequency. In the extreme case of DB localized at one light atom, it oscillates with a large amplitude,  $A$  in the anharmonic potential well, which determines its frequency  $\Omega$  as follows [19]

$$\Omega(A) = \sqrt{\alpha + \frac{3}{4}\beta A^2}, \quad \alpha = \frac{2\gamma_1}{m}, \quad \beta = \frac{2\gamma_2}{m}, \quad \gamma_1(A) = R_1A + S_1, \quad \gamma_2(A) = R_2A + S_2, \quad (9)$$

where  $\alpha$  determines the quasi-harmonic eigenfrequency of the potential well, and  $\beta$  describes its anharmonicity. Both of them depend on the DB amplitude, since it changes the force constants  $\gamma_{1,2}$  of the potential.  $\beta$  is positive, which corresponds to hard type of non-linearity with frequency increasing with  $A$ . However, the central atom oscillating with large amplitude shifts positions of neighboring atoms so that  $\alpha$  decreases with  $A$  resulting in the observed decrease of  $\Omega(A)$ [19].

Let us apply this model to a DB in the PdD lattice, dispersion curves of which [33] are shown in Fig. 3(e). Figure 4(a) shows DB $\langle 110 \rangle$  frequency  $\Omega$  and eigen frequencies of (quasi-harmonic) potential wells for neighboring D atoms,  $\omega_0$  as functions of the DB amplitude, evaluated with the force constants assumed to fit dispersion curves of PdD<sub>0.63</sub> (Fig. 3 (e)):

$$\omega_0(A) = \sqrt{\frac{2\gamma_1(A)}{m}}, \quad \gamma_1(A) = R_1A + S_1, \quad (10)$$

$$R_1 = -0.026 \text{ eV/\AA}^3, \quad S_1 = 0.008 \text{ eV/\AA}^2, \quad R_2 = -0.017 \text{ eV/\AA}^5, \quad S_2 = 0.035 \text{ eV/\AA}^4. \quad (11)$$

The frequency of the optic modes at the zone center ( $\sim 9$  THz), which determines the maximum DB frequency, is low in comparison with other hydrides, thus implying a weak nearest-neighbor Pd–D force constant in PdD<sub>0.63</sub> [33].

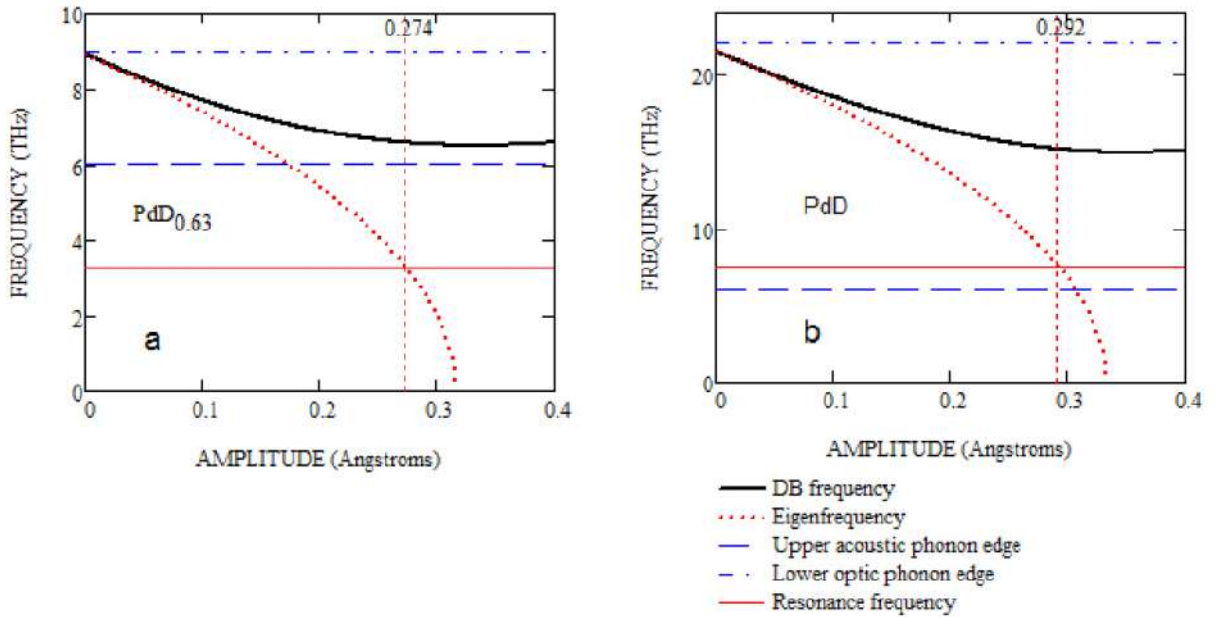


**Figure 4.** DOS of the NaCl-type crystal for the weight ratio  $m/M = 0.1$  at temperatures  $T =$ (a) 0, (b) 155, (c) 310, and (d) 620 K. (e) DOS for PdD and PdH crystals based on the force constants [33] fitted to the experimental results for PdD<sub>0.63</sub> assuming that the forces in PdD and PdD<sub>0.63</sub> were identical. Reproduced from [20,33] Copyright by APS.

Figure 4(b) shows  $\Omega(A)$  and  $\omega_0(A)$  evaluated with the force constants fitted to raise the lower optic phonon edge for stoichiometric PdD up to 22 THz and to broaden the phonon gap accordingly:

$$R_1 = -0.143 \text{ eV}/\text{\AA}^3, \quad S_1 = 0.048 \text{ eV}/\text{\AA}^2, \quad R_2 = -0.013 \text{ eV}/\text{\AA}^5, \quad S_2 = 0.143 \text{ eV}/\text{\AA}^4. \quad (12)$$

In the PdD<sub>0.63</sub> case (Fig. 4 (a)), increase of the DB amplitude up to 0.274 Å leads to the excitation in neighboring wells of the harmonic with the frequency  $\sim 3.3$  THz equal to half of the main DB frequency ( $\sim 6.6$  THz), which interacts with acoustic phonons below the gap and makes the DB unstable, similar to the NaCl case for  $m/M > 0.2$  [19].

In the PdD case (Fig. 4(b)), increase of the DB amplitude up to the critical value  $A_{\text{cr}} \approx 0.292$  Å leads to the excitation in neighboring wells of the harmonic with the frequency  $\sim 7.5$  THz equal to half of the main DB frequency ( $\sim 15$  THz), which lies above the upper acoustic phonon edge and does not interact with phonons. Such DBs are stable, and they lead to the parametric formation of CCS of deuterons in the neighboring quasi-harmonic potential wells subjected to time-periodic modulation of their eigenfrequencies  $\omega_0(A_{\text{cr}}) \approx 7.5$  THz by the DB frequency  $\Omega(A_{\text{cr}}) \approx 15$  THz. As a result of such modulation, D–D fusion is expected to occur in several dozens of DB cycles (Fig. 2(a)) since the modulation amplitude

$$g_{\Omega} \approx A_{\text{cr}} / \left( a_{\text{PdD}} \sqrt{2} / 2 \right) \approx 0.1.$$

Three main resonances of excess energy released under joint action of two low-power laser beams with variable beat frequency ranging from 3 to 24 THz at  $\sim 8 \pm 1$  THz,  $15 \pm 1$  THz and  $21 \pm 1$  THz [34] correlate in our model with the DB-induced harmonic frequency,  $\omega_0(A_{\text{cr}}) \approx 7.5$  THz, DB parametric frequency  $\Omega(A_{\text{cr}}) \approx 15$  THz and DB initial frequency, 21 THz, respectively.

#### 4. LENR Rate under Heavy Water Electrolysis

The DB excitation occurs by thermal fluctuations and by external driving displacing atoms from equilibrium positions. The rate of thermal excitation of DBs having energy  $E$  is given by the Arrhenius law [27,31]

$$K_{\text{DB}}^{\text{th}}(E) = \omega_{\text{DB}} k_{\text{DB}}^{\text{ef}} \exp\left(-\frac{E}{k_{\text{B}}T}\right), \quad (13)$$

where  $k_{\text{B}}$  is the Boltzmann constant,  $T$  is the temperature, and  $\omega_{\text{DB}} \approx \Omega(0)$  is the attempt frequency that should be close to the edge of the phonon band, from which DBs are excited. In the case of gap DBs under consideration, it is about 21 THz (Fig. 4(b)).  $k_{\text{DB}}^{\text{ef}}$  is the efficiency coefficient for the excitation of DBs with parameter fitting parametric resonance conditions.

External driving of the DB excitation can be provided by knocking of surface atoms out of equilibrium position by energetic ions or molecules under non-equilibrium deposition of deuterium under electrolysis. This produces focusing collisions and moving DBs (a.k.a. quodons) that can transfer vibration energy in the crystal bulk [25]. The amplitude of the quasi-periodic energy deviation of atoms along the quodon pathway,  $V_{\text{ex}}$ , can reach almost 1 eV with the excitation time,  $\tau_{\text{ex}}$ , of about 10 oscillation periods, which results in the amplification of the DB generation rate proportional to the electric current density  $J$  [31]:

$$K_{\text{DB}}^J(E) = K_{\text{DB}}^{\text{th}}(E) \left( 1 + \left\langle I_0 \left( \frac{V_{\text{ex}}}{k_{\text{B}}T} \right) \right\rangle \omega_{\text{ex}} \tau_{\text{ex}} \right), \quad \omega_{\text{ex}}(F_{\text{q}}) = F_{\text{q}} b^2 \frac{3l_{\text{q}}}{R_{\text{p}}}, \quad F_{\text{q}} = \frac{J}{2e}, \quad (14)$$

where  $\omega_{\text{ex}}$  is the mean number of excitations per atom per second caused by the flux of quodons,  $e$  is the electron charge,  $b$  is the atomic spacing. The product  $F_{\text{q}} b^2$  is the frequency of the excitations per atom within the layer of a thickness  $l_{\text{q}}$  equal to the quodon propagation range, while the ratio  $3l_{\text{q}}/R_{\text{p}}$  is the geometrical factor that corresponds to the relative number of atoms within the quodon range in a PdD particle of a radius  $R_{\text{p}}$ . The coefficient of proportionality

between  $F_q$  and the electron flux  $J/e$  assumes that each electrolytic reaction that involves a pair of electrons releases a vibrational energy of  $\sim 1$  eV, which is sufficient for generation of one quodon with energy  $V_{\text{ex}} < 1$  eV.

Multiplying the DB generation rate (14) by the tunneling probability in a DB,  $G^*(L, r)$  (8) and integrating over DB energies one obtains the D–D fusion rate per PdD unit cell:

$$FuR = \frac{1}{\Delta E} \int_{E_{\text{DB}}^* - \Delta E}^{E_{\text{DB}}^* + \Delta E} K_{\text{DB}}^J(E) G^*(r) dE \quad (15)$$

that dramatically depends on the correlation coefficient,  $r$ , which, in its turn, strongly depends on the DB amplitude  $\sim$  DB energy and the number of DB cycles before decay,  $n_{\text{DB}}$ .

Only a small fraction of DBs can form CCS in their vicinity and act as effective *breather nano-colliders* (BNC). They must have some particular energies,  $E_{\text{DB}}^* \pm \Delta E$ , in order to cause the parametric resonance producing CCS. If  $\Delta E \ll k_B T$  Eq. (15) is reduced to

$$FuR \approx 2K_{\text{DB}}^J(E_{\text{DB}}^*) G^*(r(E_{\text{DB}}^*, n_{\text{DB}}^*)) \xrightarrow{n_{\text{DB}} > n_{\text{DB}}^*} K_{\text{DB}}^J(E_{\text{DB}}^*), \quad G^*(r(E_{\text{DB}}^*, n_{\text{DB}}^*)) \approx \frac{1}{2}, \quad (16)$$

where the number of DB cycles required to make the Coulomb barrier ‘transparent’,  $n_{\text{DB}}^* \approx 100$  at  $g_{\Omega} = 0.1$ .

We consider the following reaction [2]:  $D + D \rightarrow {}^4\text{He} + 23.8 \text{ MeV}_{\text{lattice}}$ , which is based on the experimentally observed production of excess heat correlated with production of “nuclear ash”, i.e.  ${}^4\text{He}$  [2,3]. Multiplying the DB-induced fusion rate (16) by the energy  $E_{\text{D-D}} = 23.8 \text{ MeV}$ , produced in D–D fusion one obtains the excess energy production rate per atom,  $P_{\text{D-D}}$  as a function of temperature and electric current:  $P_{\text{D-D}}(T, J) = K_{\text{DB}}^J(E_{\text{DB}}^*, T, J) E_{\text{D-D}}$ . Usually, the output power density is measured per unite surface of a macroscopic cell,  $P_{\text{D-D}}^S$ , as a function of the electric current density at a fixed temperature and at temperature increasing with  $J$ , as illustrated in Fig. 5. This is given by the product of  $P_{\text{D-D}}$ , the number of atoms per unit volume,  $1/v_{\text{PdD}}$  ( $v_{\text{PdD}}$  being the atomic volume of PdD) and the ratio of the cell volume to the cell surface:

$$P_{\text{D-D}}^S(T, J) = P_{\text{D-D}}(T, J) \frac{L_S}{v_{\text{PdD}}}, \quad (17)$$

where  $L_S$  is the cell size, if cubic, or thickness, in case of a plate .

Figure 5 shows the LENR output power density DBs as a function of electric current density and temperature evaluated by Eq. (17) assuming material parameters listed in Table 1. Comparison with experimental data shows that the present model describes quantitatively the observed linear dependence of  $P_{\text{D-D}}^S$  on the current density at a constant temperature as well as the deviation from the linear dependence, if temperature increases with increasing electric current density. Thermally activated nature of the reactions leading to LENR has been noted for quite a long time [3], and the activation energy was estimated in some cases to be  $\sim 0.65$  eV. The present model not only explains these observations, but also reveals that the underlying physics is a consequence of the synergy between thermally activated and externally driven mechanisms of the DB excitation in deuterated palladium.

## 5. Conclusions and Outlook

The main message of this paper is that DBs present the most efficient way to produce CCS due to time-periodic modulation of the potential well width (or the Coulomb barrier width) and hence to act as BNC triggering LENR in solids. The BNC concept proposed in a previous work [31] did not take into account correlation effects, and hence, unrealistically small separation between atoms ( $\sim 0.01 \text{ \AA}$ ) would have to be attained in order to enhance the LENR rate up to a noticeable level. Figure 2 demonstrates effect of CCS in the BNC model manifested by a number of DB

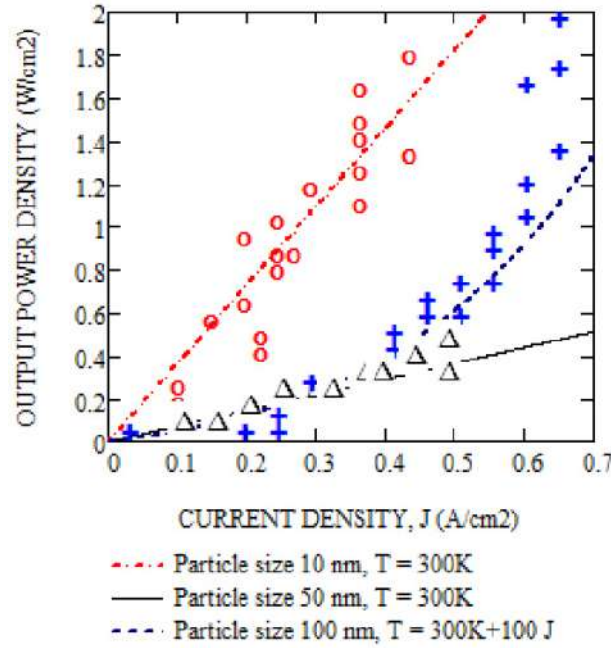


**Figure 5.** LENR output power density according to the model Eq. (17) and material parameters listed in the table as a function of electric current density at constant  $T$  and  $T$  increasing with  $J$  as  $T = 300\text{K} + 100J$ . Experimental data [3] Fig. 42:  $\circ$  - Bush (constant  $T$ ),  $\Delta$  - Storms (constant  $T$ ),  $+$  Aoki et al. ( $T$  increasing with  $J$ ).

cycles required to produce experimentally observed LENR rate  $\sim 1 \text{ W/cm}^2$ . It can be seen that in the modified model, the DB lifetime plays a much more important role than the tunneling D–D spacing, and that DB amplitude of several fractions of an angstrom is sufficient to produce the required effect, if CCS parametric conditions are met.

The present model describes the observed linear dependence of the excess power output on the current density under heavy water electrolysis at a constant temperature, as well as its exponential increase with increasing temperature, which can be the basic LENR mechanism in the hot CAT-type installations.

**Table 1.** Material parameters used for the plot in Fig. 5.

Parameter	Value
D–D spacing in PdD, $b$ (Å)	0.29
DB parametric amplitude, $A_{cr}$ (Å)	0.292
DB parametric energy, $E_{DB}^*$ (eV)	1
DB initial frequency, $\Omega(0)$ (THz)	21
DB parametric freq, $\Omega(A_{cr})$ (THz)	15
Harmonic frequency $\omega_0(A_{cr})$ (THz)	7.5
DB lifetime, $\tau_{DB}^* = n_{DB}^*/\omega_{DB}$ (s)	$6 \times 10^{-12}$
DB excitation efficiency, $k_{DB}^{ef}$	$4 \times 10^{-11}$
Quodon excitation energy $V_{ex}$ (eV)	0.8
Quodon excitation time, $\tau_{ex}$ (s)	$6 \times 10^{-13}$
Quodon range, $l_q = 10b$ (nm)	2.9
Cathode size/thickness (mm)	5

The proposed mechanism of CCS formation near the gap DBs requires a sufficiently broad phonon gap that is not observed below the critical D loading  $\sim 0.83$  examined so far. Our hypothesis is that mechanical stresses arising in a fine powder of PdD<sub>x</sub> above the critical loading  $x > 0.83$  can make the phonon band similar to that shown in Fig. 4(b), thus switching on the DB-induced formation of CCS. Further investigations of DOS and DBs in the extreme conditions of LENR are required.

An alternative mechanism of the DB-induced CCS formation may involve high frequency (hard type) DBs, manifested by the peak *above* the phonon spectrum in NaCl type crystals. Atomic modeling of DBs of various types in metal hydrides/deuterides is an important outstanding problem since it may offer ways of *engineering* the nuclear active environment.

### Acknowledgements

The author is grateful to Sergey Dmitriev and Vladimir Vysotskii for helpful discussions and valuable criticism.

### References

- [1] M. Fleischmann, S. Pons and M. Hawkins, *J. Electroanal. Chem.* **261** (1989) 301.
- [2] M. McKubre, F. Tanzella, P. Hagelstein, K. Mullican and M. Trevithick, The need for triggering in cold fusion reactions, in *10th Int. Conf. on Cold Fusion*, MA, Cambridge, 2003, LENR-CANR.org.
- [3] E.K Storms, *The Science of Low Energy Nuclear Reaction*, World Scientific, Singapore, 2007.
- [4] A.G. Parkhomov, *Int. J. Unconventional Sci.* **7**(3) (2015) 68.
- [5] H.J. Assenbaum, K. Langanke and C. Rolfs, *Z. Phys. A* **327** (1987) 461.
- [6] J. Kasagi, Screening potential for nuclear reactions in condensed matter, in *ICCF-14 Int. Conf. on Condensed Matter Nucl. Sci.*, 2008.
- [7] E. Schrödinger, *Ber. Kgl. Akad. Wiss., Berlin, S.* (1930) 296.
- [8] H.P. Robertson, *Phys. Rev.* **34** (1930) 163.
- [9] V.V. Dodonov and V.I. Man'ko, *Phys. Lett. A* **79**(2/3) (1980) 150.
- [10] V.I. Vysotskii and S.V. Adamenko, *J. Tech. Phys.* **55** (2010) 613.
- [11] V.I. Vysotskii, M.V. Vysotskyy and S.V. Adamenko, *J. Exp. Theoret. Phys.* **141** (2012) 276.
- [12] V.I. Vysotskii, S.V. Adamenko and M.V. Vysotskyy, *J. Exp. Theoret. Phys.* **142** (2012) 627.
- [13] V.I. Vysotskii and M.V. Vysotskyy, *Euro. Phys. J. A* **49**(8) (2013) 1–12, DOI 10.1140/epja/i2013-13099-2.
- [14] A.J. Sievers and S. Takeno, *Phys. Rev. Lett.* **61** (1988) 970.
- [15] S. Flach and A.V. Gorbach, *Phys. Rep.* **467** (2008) 1.
- [16] V. Hizhnyakov, D. Nevedrov and A.J. Sievers, *Physica B*, **316–317** (2002) 132.
- [17] M.E. Manley, A.J. Sievers, J.W. Lynn, S.A. Kiselev, N.I. Agladze, Y. Chen, A. Llobet and A. Alatas, *Phys. Rev. B* **79** (2009) 134304.
- [18] M.E. Manley, *Acta Materialia* **58** (2010) 2926.
- [19] L.Z. Khadeeva and S.V. Dmitriev, *Phys. Rev. B* **81** (2010) 214306.
- [20] A.A. Kistanov and S.V. Dmitriev, *Phys. Solid State* **54** (2012) 1648.
- [21] L.Z. Khadeeva and S.V. Dmitriev, *Phys. Rev. B*, **84** (2011) 144304.
- [22] S.V. Dmitriev, A.P. Chetverikov and M.G. Velarde, *Physica Status Solidi (b)* **54** (2015) 1648.
- [23] N.K. Voulgarakis, G. Hadjisavvas, P.C. Kelires and G.P. Tsironis, *Phys. Rev. B* **69** (2004) 113201.
- [24] M. Haas, V. Hizhnyakov, A. Shelkan, M. Klopov and A.J. Sievers, *Phys. Rev. B* **84** (2011) 14430.
- [25] D. Terentyev, A. Dubinko, V. Dubinko, S. Dmitriev, E. Zhurkin and M. Sorokin, Interaction of discrete breathers with primary lattice defects in bcc Fe, *Modelling Simul. Mater. Sci. Eng.* **23** (2015) 085007-085030.
- [26] F. Piazza and Y.H. Sanejouand, *Phys. Biol.* **5** (2008) 026001.
- [27] V.I. Dubinko, P.A. Selyshev and J.F.R. Archilla, *Phys. Rev. E* **83**(4) (2011) 041124.
- [28] V.I. Dubinko, F.M. Russell, *J. Nucl. Materials* **419** (2011) 378.

- [29] V.I. Dubinko and A.V. Dubinko, *Nucl. Inst. and Methods in Phys. Res. B* **303** (2013) 133.
- [30] V.I. Dubinko and F. Piazza, *Lett. Materials* **4** (4) (2014) 273.
- [31] V.I. Dubinko, *J. Condensed Matter Nucl. Sci.* **14** (2014) 87.
- [32] J.M. Rowe, J.J. Rush, H.G. Smith, M. Mostoller and H.E. Flotow, *Phys. Rev. Lett.* **33** (1974) 1297.
- [33] I. Errea, M. Calandra<sup>1</sup> and F. Mauri, *Phys. Rev. Lett.* **111** (2013) 177002.
- [34] P.L. Hagelstein, D. Letts and D. Cravens, *J. Condensed Matter Nucl. Sci.* **3** (2010) 59–76.